

Observation of the Decay $B^0 \rightarrow \pi^0 \pi^0$

B. Aubert,¹ R. Barate,¹ D. Boutigny,¹ J.-M. Gaillard,¹ A. Hicheur,¹ Y. Karyotakis,¹ J. P. Lees,¹ P. Robbe,¹
V. Tisserand,¹ A. Zghiche,¹ A. Palano,² A. Pompili,² J. C. Chen,³ N. D. Qi,³ G. Rong,³ P. Wang,³ Y. S. Zhu,³
G. Eigen,⁴ I. Ofte,⁴ B. Stugu,⁴ G. S. Abrams,⁵ A. W. Borgland,⁵ A. B. Breon,⁵ D. N. Brown,⁵ J. Button-Shafer,⁵
R. N. Cahn,⁵ E. Charles,⁵ C. T. Day,⁵ M. S. Gill,⁵ A. V. Gritsan,⁵ Y. Groysman,⁵ R. G. Jacobsen,⁵ R. W. Kadel,⁵
J. Kadyk,⁵ L. T. Kerth,⁵ Yu. G. Kolomensky,⁵ J. F. Kral,⁵ G. Kukartsev,⁵ C. LeClerc,⁵ M. E. Levi,⁵ G. Lynch,⁵
L. M. Mir,⁵ P. J. Oddone,⁵ T. J. Orimoto,⁵ M. Pripstein,⁵ N. A. Roe,⁵ A. Romosan,⁵ M. T. Ronan,⁵ V. G. Shelkov,⁵
A. V. Telnov,⁵ W. A. Wenzel,⁵ K. Ford,⁶ T. J. Harrison,⁶ C. M. Hawkes,⁶ D. J. Knowles,⁶ S. E. Morgan,⁶
R. C. Penny,⁶ A. T. Watson,⁶ N. K. Watson,⁶ K. Goetzen,⁷ T. Held,⁷ H. Koch,⁷ B. Lewandowski,⁷ M. Pelizaeus,⁷
K. Peters,⁷ H. Schmuecker,⁷ M. Steinke,⁷ N. R. Barlow,⁸ J. T. Boyd,⁸ N. Chevalier,⁸ W. N. Cottingham,⁸
M. P. Kelly,⁸ T. E. Latham,⁸ C. Mackay,⁸ F. F. Wilson,⁸ K. Abe,⁹ T. Cuhadar-Donszelmann,⁹ C. Hearty,⁹
T. S. Mattison,⁹ J. A. McKenna,⁹ D. Thiessen,⁹ P. Kyberd,¹⁰ A. K. McKemey,¹⁰ V. E. Blinov,¹¹ A. D. Bukin,¹¹
V. B. Golubev,¹¹ V. N. Ivanchenko,¹¹ E. A. Kravchenko,¹¹ A. P. Onuchin,¹¹ S. I. Serednyakov,¹¹ Yu. I. Skovpen,¹¹
E. P. Solodov,¹¹ A. N. Yushkov,¹¹ D. Best,¹² M. Bruinsma,¹² M. Chao,¹² D. Kirkby,¹² A. J. Lankford,¹²
M. Mandelkern,¹² R. K. Mommsen,¹² W. Roethel,¹² D. P. Stoker,¹² C. Buchanan,¹³ B. L. Hartfiel,¹³ B. C. Shen,¹⁴
D. del Re,¹⁵ H. K. Hadavand,¹⁵ E. J. Hill,¹⁵ D. B. MacFarlane,¹⁵ H. P. Paar,¹⁵ Sh. Rahatlou,¹⁵ V. Sharma,¹⁵
J. W. Berryhill,¹⁶ C. Campagnari,¹⁶ B. Dahmes,¹⁶ N. Kuznetsova,¹⁶ S. L. Levy,¹⁶ O. Long,¹⁶ A. Lu,¹⁶
M. A. Mazur,¹⁶ J. D. Richman,¹⁶ W. Verkerke,¹⁶ T. W. Beck,¹⁷ J. Beringer,¹⁷ A. M. Eisner,¹⁷ C. A. Heusch,¹⁷
W. S. Lockman,¹⁷ T. Schalk,¹⁷ R. E. Schmitz,¹⁷ B. A. Schumm,¹⁷ A. Seiden,¹⁷ M. Turri,¹⁷ W. Walkowiak,¹⁷
D. C. Williams,¹⁷ M. G. Wilson,¹⁷ J. Albert,¹⁸ E. Chen,¹⁸ G. P. Dubois-Felsmann,¹⁸ A. Dvoretzskii,¹⁸ D. G. Hitlin,¹⁸
I. Narsky,¹⁸ F. C. Porter,¹⁸ A. Ryd,¹⁸ A. Samuel,¹⁸ S. Yang,¹⁸ S. Jayatilleke,¹⁹ G. Mancinelli,¹⁹ B. T. Meadows,¹⁹
M. D. Sokoloff,¹⁹ T. Abe,²⁰ F. Blanc,²⁰ P. Bloom,²⁰ S. Chen,²⁰ P. J. Clark,²⁰ W. T. Ford,²⁰ U. Nauenberg,²⁰
A. Olivas,²⁰ P. Rankin,²⁰ J. Roy,²⁰ J. G. Smith,²⁰ W. C. van Hoek,²⁰ L. Zhang,²⁰ J. L. Harton,²¹ T. Hu,²¹
A. Soffer,²¹ W. H. Toki,²¹ R. J. Wilson,²¹ J. Zhang,²¹ D. Altenburg,²² T. Brandt,²² J. Brose,²² T. Colberg,²²
M. Dickopp,²² R. S. Dubitzky,²² A. Hauke,²² H. M. Lacker,²² E. Maly,²² R. Müller-Pfefferkorn,²² R. Nogowski,²²
S. Otto,²² J. Schubert,²² K. R. Schubert,²² R. Schwierz,²² B. Spaan,²² L. Wilden,²² D. Bernard,²³
G. R. Bonneaud,²³ F. Brochard,²³ J. Cohen-Tanugi,²³ P. Grenier,²³ Ch. Thiebaux,²³ G. Vasileiadis,²³ M. Verderi,²³
A. Khan,²⁴ D. Lavin,²⁴ F. Muheim,²⁴ S. Playfer,²⁴ J. E. Swain,²⁴ M. Andreotti,²⁵ V. Azzolini,²⁵ D. Bettoni,²⁵
C. Bozzi,²⁵ R. Calabrese,²⁵ G. Cibinetto,²⁵ E. Luppi,²⁵ M. Negrini,²⁵ L. Piemontese,²⁵ A. Sarti,²⁵ E. Treadwell,²⁶
F. Anulli,²⁷ * R. Baldini-Ferroli,²⁷ M. Biasini,²⁷ * A. Calcaterra,²⁷ R. de Sangro,²⁷ D. Falciari,²⁷ G. Finocchiaro,²⁷
P. Patteri,²⁷ I. M. Peruzzi,²⁷ * M. Piccolo,²⁷ M. Pioppi,²⁷ * A. Zallo,²⁷ A. Buzzo,²⁸ R. Capra,²⁸ R. Contri,²⁸
G. Crosetti,²⁸ M. Lo Vetere,²⁸ M. Macri,²⁸ M. R. Monge,²⁸ S. Passaggio,²⁸ C. Patrignani,²⁸ E. Robutti,²⁸
A. Santroni,²⁸ S. Tosi,²⁸ S. Bailey,²⁹ M. Morii,²⁹ E. Won,²⁹ W. Bhimji,³⁰ D. A. Bowerman,³⁰ P. D. Dauncey,³⁰
U. Egede,³⁰ I. Eschrich,³⁰ J. R. Gaillard,³⁰ G. W. Morton,³⁰ J. A. Nash,³⁰ P. Sanders,³⁰ G. P. Taylor,³⁰
G. J. Grenier,³¹ S.-J. Lee,³¹ U. Mallik,³¹ J. Cochran,³² H. B. Crawley,³² J. Lamsa,³² W. T. Meyer,³² S. Prell,³²
E. I. Rosenberg,³² J. Yi,³² M. Davier,³³ G. Grosdidier,³³ A. Höcker,³³ S. Laplace,³³ F. Le Diberder,³³ V. Lepeltier,³³
A. M. Lutz,³³ T. C. Petersen,³³ S. Plaszczynski,³³ M. H. Schune,³³ L. Tantot,³³ G. Wormser,³³ V. Brigljević,³⁴
C. H. Cheng,³⁴ D. J. Lange,³⁴ D. M. Wright,³⁴ A. J. Bevan,³⁵ J. P. Coleman,³⁵ J. R. Fry,³⁵ E. Gabathuler,³⁵
R. Gamet,³⁵ M. Kay,³⁵ R. J. Parry,³⁵ D. J. Payne,³⁵ R. J. Sloane,³⁵ C. Touramanis,³⁵ J. J. Back,³⁶ P. F. Harrison,³⁶
H. W. Shorthouse,³⁶ P. Strother,³⁶ P. B. Vidal,³⁶ C. L. Brown,³⁷ G. Cowan,³⁷ R. L. Flack,³⁷ H. U. Flaecher,³⁷
S. George,³⁷ M. G. Green,³⁷ A. Kurup,³⁷ C. E. Marker,³⁷ T. R. McMahon,³⁷ S. Ricciardi,³⁷ F. Salvatore,³⁷
G. Vaitsas,³⁷ M. A. Winter,³⁷ D. Brown,³⁸ C. L. Davis,³⁸ J. Allison,³⁹ R. J. Barlow,³⁹ A. C. Forti,³⁹ P. A. Hart,³⁹
M. C. Hodgkinson,³⁹ F. Jackson,³⁹ G. D. Lafferty,³⁹ A. J. Lyon,³⁹ J. H. Weatherall,³⁹ J. C. Williams,³⁹ A. Farbin,⁴⁰
A. Jawahery,⁴⁰ D. Kovalskyi,⁴⁰ C. K. Lae,⁴⁰ V. Lillard,⁴⁰ D. A. Roberts,⁴⁰ G. Blaylock,⁴¹ C. Dallapiccola,⁴¹
K. T. Flood,⁴¹ S. S. Hertzbach,⁴¹ R. Kofler,⁴¹ V. B. Koptchev,⁴¹ T. B. Moore,⁴¹ S. Saremi,⁴¹ H. Staengle,⁴¹
S. Willocq,⁴¹ R. Cowan,⁴² G. Sciolla,⁴² F. Taylor,⁴² R. K. Yamamoto,⁴² D. J. J. Mangeol,⁴³ P. M. Patel,⁴³
A. Lazzaro,⁴⁴ F. Palombo,⁴⁴ J. M. Bauer,⁴⁵ L. Cremaldi,⁴⁵ V. Eschenburg,⁴⁵ R. Godang,⁴⁵ R. Kroeger,⁴⁵

J. Reidy,⁴⁵ D. A. Sanders,⁴⁵ D. J. Summers,⁴⁵ H. W. Zhao,⁴⁵ S. Brunet,⁴⁶ D. Cote-Ahern,⁴⁶ C. Hast,⁴⁶ P. Taras,⁴⁶ H. Nicholson,⁴⁷ C. Cartaro,⁴⁸ N. Cavallo,^{48,†} G. De Nardo,⁴⁸ F. Fabozzi,^{48,†} C. Gatto,⁴⁸ L. Lista,⁴⁸ P. Paolucci,⁴⁸ D. Piccolo,⁴⁸ C. Sciacca,⁴⁸ M. A. Baak,⁴⁹ G. Raven,⁴⁹ J. M. LoSecco,⁵⁰ T. A. Gabriel,⁵¹ B. Brau,⁵² K. K. Gan,⁵² K. Honscheid,⁵² D. Hufnagel,⁵² H. Kagan,⁵² R. Kass,⁵² T. Pulliam,⁵² Q. K. Wong,⁵² J. Brau,⁵³ R. Frey,⁵³ C. T. Potter,⁵³ N. B. Sinev,⁵³ D. Strom,⁵³ E. Torrence,⁵³ F. Colecchia,⁵⁴ A. Dorigo,⁵⁴ F. Galeazzi,⁵⁴ M. Margoni,⁵⁴ M. Morandin,⁵⁴ M. Posocco,⁵⁴ M. Rotondo,⁵⁴ F. Simonetto,⁵⁴ R. Stroili,⁵⁴ G. Tiozzo,⁵⁴ C. Voci,⁵⁴ M. Benayoun,⁵⁵ H. Briand,⁵⁵ J. Chauveau,⁵⁵ P. David,⁵⁵ Ch. de la Vaissière,⁵⁵ L. Del Buono,⁵⁵ O. Hamon,⁵⁵ M. J. J. John,⁵⁵ Ph. Leruste,⁵⁵ J. Ocariz,⁵⁵ M. Pivk,⁵⁵ L. Roos,⁵⁵ J. Stark,⁵⁵ S. T'Jampens,⁵⁵ G. Therin,⁵⁵ P. F. Manfredi,⁵⁶ V. Re,⁵⁶ P. K. Behera,⁵⁷ L. Gladney,⁵⁷ Q. H. Guo,⁵⁷ J. Panetta,⁵⁷ C. Angelini,⁵⁸ G. Batignani,⁵⁸ S. Bettarini,⁵⁸ M. Bondioli,⁵⁸ F. Bucci,⁵⁸ G. Calderini,⁵⁸ M. Carpinelli,⁵⁸ V. Del Gamba,⁵⁸ F. Forti,⁵⁸ M. A. Giorgi,⁵⁸ A. Lusiani,⁵⁸ G. Marchiori,⁵⁸ F. Martinez-Vidal,^{58,‡} M. Morganti,⁵⁸ N. Neri,⁵⁸ E. Paoloni,⁵⁸ M. Rama,⁵⁸ G. Rizzo,⁵⁸ F. Sandrelli,⁵⁸ J. Walsh,⁵⁸ M. Haire,⁵⁹ D. Judd,⁵⁹ K. Paick,⁵⁹ D. E. Wagoner,⁵⁹ N. Danielson,⁶⁰ P. Elmer,⁶⁰ C. Lu,⁶⁰ V. Miftakov,⁶⁰ J. Olsen,⁶⁰ A. J. S. Smith,⁶⁰ H. A. Tanaka,⁶⁰ E. W. Varnes,⁶⁰ F. Bellini,⁶¹ G. Cavoto,^{60,61} R. Faccini,^{15,61} F. Ferrarotto,⁶¹ F. Ferroni,⁶¹ M. Gaspero,⁶¹ M. A. Mazzoni,⁶¹ S. Morganti,⁶¹ M. Pierini,⁶¹ G. Piredda,⁶¹ F. Safai Tehrani,⁶¹ C. Voena,⁶¹ S. Christ,⁶² G. Wagner,⁶² R. Waldi,⁶² T. Adye,⁶³ N. De Groot,⁶³ B. Franek,⁶³ N. I. Geddes,⁶³ G. P. Gopal,⁶³ E. O. Olaiya,⁶³ S. M. Xella,⁶³ R. Aleksan,⁶⁴ S. Emery,⁶⁴ A. Gaidot,⁶⁴ S. F. Ganzhur,⁶⁴ P.-F. Giraud,⁶⁴ G. Hamel de Monchenault,⁶⁴ W. Kozanecki,⁶⁴ M. Langer,⁶⁴ M. Legendre,⁶⁴ G. W. London,⁶⁴ B. Mayer,⁶⁴ G. Schott,⁶⁴ G. Vasseur,⁶⁴ Ch. Yeche,⁶⁴ M. Zito,⁶⁴ M. V. Purohit,⁶⁵ A. W. Weidemann,⁶⁵ F. X. Yumiceva,⁶⁵ D. Aston,⁶⁶ R. Bartoldus,⁶⁶ N. Berger,⁶⁶ A. M. Boyarski,⁶⁶ O. L. Buchmueller,⁶⁶ M. R. Convery,⁶⁶ D. P. Coupal,⁶⁶ D. Dong,⁶⁶ J. Dorfan,⁶⁶ D. Dujmic,⁶⁶ W. Dunwoodie,⁶⁶ R. C. Field,⁶⁶ T. Glanzman,⁶⁶ S. J. Gowdy,⁶⁶ E. Grauges-Pous,⁶⁶ T. Hadig,⁶⁶ V. Halys,⁶⁶ T. Hryn'ova,⁶⁶ W. R. Innes,⁶⁶ C. P. Jessop,⁶⁶ M. H. Kelsey,⁶⁶ P. Kim,⁶⁶ M. L. Kocian,⁶⁶ U. Langenegger,⁶⁶ D. W. G. S. Leith,⁶⁶ S. Luitz,⁶⁶ V. Luth,⁶⁶ H. L. Lynch,⁶⁶ H. Marsiske,⁶⁶ R. Messner,⁶⁶ D. R. Muller,⁶⁶ C. P. O'Grady,⁶⁶ V. E. Ozcan,⁶⁶ A. Perazzo,⁶⁶ M. Perl,⁶⁶ S. Petrak,⁶⁶ B. N. Ratcliff,⁶⁶ S. H. Robertson,⁶⁶ A. Roodman,⁶⁶ A. A. Salnikov,⁶⁶ R. H. Schindler,⁶⁶ J. Schwiening,⁶⁶ G. Simi,⁶⁶ A. Snyder,⁶⁶ A. Soha,⁶⁶ J. Stelzer,⁶⁶ D. Su,⁶⁶ M. K. Sullivan,⁶⁶ J. Va'vra,⁶⁶ S. R. Wagner,⁶⁶ M. Weaver,⁶⁶ A. J. R. Weinstein,⁶⁶ W. J. Wisniewski,⁶⁶ D. H. Wright,⁶⁶ C. C. Young,⁶⁶ P. R. Burchat,⁶⁷ A. J. Edwards,⁶⁷ T. I. Meyer,⁶⁷ B. A. Petersen,⁶⁷ C. Roat,⁶⁷ S. Ahmed,⁶⁸ M. S. Alam,⁶⁸ J. A. Ernst,⁶⁸ M. Saleem,⁶⁸ F. R. Wappler,⁶⁸ W. Bugg,⁶⁹ M. Krishnamurthy,⁶⁹ S. M. Spanier,⁶⁹ R. Eckmann,⁷⁰ H. Kim,⁷⁰ J. L. Ritchie,⁷⁰ R. F. Schwitters,⁷⁰ J. M. Izen,⁷¹ I. Kitayama,⁷¹ X. C. Lou,⁷¹ S. Ye,⁷¹ F. Bianchi,⁷² M. Bona,⁷² F. Gallo,⁷² D. Gamba,⁷² C. Borean,⁷³ L. Bosisio,⁷³ G. Della Ricca,⁷³ S. Dittongo,⁷³ S. Grancagnolo,⁷³ L. Lancieri,⁷³ P. Poropat,^{73,§} L. Vitale,⁷³ G. Vuagnin,⁷³ R. S. Panvini,⁷⁴ Sw. Banerjee,⁷⁵ C. M. Brown,⁷⁵ D. Fortin,⁷⁵ P. D. Jackson,⁷⁵ R. Kowalewski,⁷⁵ J. M. Roney,⁷⁵ H. R. Band,⁷⁶ S. Dasu,⁷⁶ M. Datta,⁷⁶ A. M. Eichenbaum,⁷⁶ J. R. Johnson,⁷⁶ P. E. Kutter,⁷⁶ H. Li,⁷⁶ R. Liu,⁷⁶ F. Di Lodovico,⁷⁶ A. Mihalyi,⁷⁶ A. K. Mohapatra,⁷⁶ Y. Pan,⁷⁶ R. Prepost,⁷⁶ S. J. Sekula,⁷⁶ J. H. von Wimmersperg-Toeller,⁷⁶ J. Wu,⁷⁶ S. L. Wu,⁷⁶ Z. Yu,⁷⁶ and H. Neal⁷⁷

(The BABAR Collaboration)

¹Laboratoire de Physique des Particules, F-74941 Annecy-le-Vieux, France

²Università di Bari, Dipartimento di Fisica and INFN, I-70126 Bari, Italy

³Institute of High Energy Physics, Beijing 100039, China

⁴University of Bergen, Inst. of Physics, N-5007 Bergen, Norway

⁵Lawrence Berkeley National Laboratory and University of California, Berkeley, CA 94720, USA

⁶University of Birmingham, Birmingham, B15 2TT, United Kingdom

⁷Ruhr Universität Bochum, Institut für Experimentalphysik 1, D-44780 Bochum, Germany

⁸University of Bristol, Bristol BS8 1TL, United Kingdom

⁹University of British Columbia, Vancouver, BC, Canada V6T 1Z1

¹⁰Brunel University, Uxbridge, Middlesex UB8 3PH, United Kingdom

¹¹Budker Institute of Nuclear Physics, Novosibirsk 630090, Russia

¹²University of California at Irvine, Irvine, CA 92697, USA

¹³University of California at Los Angeles, Los Angeles, CA 90024, USA

¹⁴University of California at Riverside, Riverside, CA 92521, USA

¹⁵University of California at San Diego, La Jolla, CA 92093, USA

¹⁶University of California at Santa Barbara, Santa Barbara, CA 93106, USA

¹⁷University of California at Santa Cruz, Institute for Particle Physics, Santa Cruz, CA 95064, USA

¹⁸California Institute of Technology, Pasadena, CA 91125, USA

¹⁹University of Cincinnati, Cincinnati, OH 45221, USA

²⁰University of Colorado, Boulder, CO 80309, USA

- ²¹Colorado State University, Fort Collins, CO 80523, USA
- ²²Technische Universität Dresden, Institut für Kern- und Teilchenphysik, D-01062 Dresden, Germany
- ²³Ecole Polytechnique, LLR, F-91128 Palaiseau, France
- ²⁴University of Edinburgh, Edinburgh EH9 3JZ, United Kingdom
- ²⁵Università di Ferrara, Dipartimento di Fisica and INFN, I-44100 Ferrara, Italy
- ²⁶Florida A&M University, Tallahassee, FL 32307, USA
- ²⁷Laboratori Nazionali di Frascati dell'INFN, I-00044 Frascati, Italy
- ²⁸Università di Genova, Dipartimento di Fisica and INFN, I-16146 Genova, Italy
- ²⁹Harvard University, Cambridge, MA 02138, USA
- ³⁰Imperial College London, London, SW7 2BW, United Kingdom
- ³¹University of Iowa, Iowa City, IA 52242, USA
- ³²Iowa State University, Ames, IA 50011-3160, USA
- ³³Laboratoire de l'Accélérateur Linéaire, F-91898 Orsay, France
- ³⁴Lawrence Livermore National Laboratory, Livermore, CA 94550, USA
- ³⁵University of Liverpool, Liverpool L69 3BX, United Kingdom
- ³⁶Queen Mary, University of London, E1 4NS, United Kingdom
- ³⁷University of London, Royal Holloway and Bedford New College, Egham, Surrey TW20 0EX, United Kingdom
- ³⁸University of Louisville, Louisville, KY 40292, USA
- ³⁹University of Manchester, Manchester M13 9PL, United Kingdom
- ⁴⁰University of Maryland, College Park, MD 20742, USA
- ⁴¹University of Massachusetts, Amherst, MA 01003, USA
- ⁴²Massachusetts Institute of Technology, Laboratory for Nuclear Science, Cambridge, MA 02139, USA
- ⁴³McGill University, Montréal, QC, Canada H3A 2T8
- ⁴⁴Università di Milano, Dipartimento di Fisica and INFN, I-20133 Milano, Italy
- ⁴⁵University of Mississippi, University, MS 38677, USA
- ⁴⁶Université de Montréal, Laboratoire René J. A. Lévesque, Montréal, QC, Canada H3C 3J7
- ⁴⁷Mount Holyoke College, South Hadley, MA 01075, USA
- ⁴⁸Università di Napoli Federico II, Dipartimento di Scienze Fisiche and INFN, I-80126, Napoli, Italy
- ⁴⁹NIKHEF, National Institute for Nuclear Physics and High Energy Physics, NL-1009 DB Amsterdam, The Netherlands
- ⁵⁰University of Notre Dame, Notre Dame, IN 46556, USA
- ⁵¹Oak Ridge National Laboratory, Oak Ridge, TN 37831, USA
- ⁵²Ohio State University, Columbus, OH 43210, USA
- ⁵³University of Oregon, Eugene, OR 97403, USA
- ⁵⁴Università di Padova, Dipartimento di Fisica and INFN, I-35131 Padova, Italy
- ⁵⁵Universités Paris VI et VII, Lab de Physique Nucléaire H. E., F-75252 Paris, France
- ⁵⁶Università di Pavia, Dipartimento di Elettronica and INFN, I-27100 Pavia, Italy
- ⁵⁷University of Pennsylvania, Philadelphia, PA 19104, USA
- ⁵⁸Università di Pisa, Dipartimento di Fisica, Scuola Normale Superiore and INFN, I-56127 Pisa, Italy
- ⁵⁹Prairie View A&M University, Prairie View, TX 77446, USA
- ⁶⁰Princeton University, Princeton, NJ 08544, USA
- ⁶¹Università di Roma La Sapienza, Dipartimento di Fisica and INFN, I-00185 Roma, Italy
- ⁶²Universität Rostock, D-18051 Rostock, Germany
- ⁶³Rutherford Appleton Laboratory, Chilton, Didcot, Oxon, OX11 0QX, United Kingdom
- ⁶⁴DSM/Dapnia, CEA/Saclay, F-91191 Gif-sur-Yvette, France
- ⁶⁵University of South Carolina, Columbia, SC 29208, USA
- ⁶⁶Stanford Linear Accelerator Center, Stanford, CA 94309, USA
- ⁶⁷Stanford University, Stanford, CA 94305-4060, USA
- ⁶⁸State Univ. of New York, Albany, NY 12222, USA
- ⁶⁹University of Tennessee, Knoxville, TN 37996, USA
- ⁷⁰University of Texas at Austin, Austin, TX 78712, USA
- ⁷¹University of Texas at Dallas, Richardson, TX 75083, USA
- ⁷²Università di Torino, Dipartimento di Fisica Sperimentale and INFN, I-10125 Torino, Italy
- ⁷³Università di Trieste, Dipartimento di Fisica and INFN, I-34127 Trieste, Italy
- ⁷⁴Vanderbilt University, Nashville, TN 37235, USA
- ⁷⁵University of Victoria, Victoria, BC, Canada V8W 3P6
- ⁷⁶University of Wisconsin, Madison, WI 53706, USA
- ⁷⁷Yale University, New Haven, CT 06511, USA

(Dated: June 7, 2018)

We present an observation of the decay $B^0 \rightarrow \pi^0 \pi^0$ based on a sample of 124 million $B\bar{B}$ pairs recorded by the BABAR detector at the PEP-II asymmetric-energy B Factory at SLAC. We observe $46 \pm 13 \pm 3$ events, where the first error is statistical and the second is systematic, corresponding to a significance of 4.2 standard deviations including systematic uncertainties. We measure the branching fraction $\mathcal{B}(B^0 \rightarrow \pi^0 \pi^0) = (2.1 \pm 0.6 \pm 0.3) \times 10^{-6}$, averaged over B^0 and \bar{B}^0 decays.

The study of B meson decays into charmless hadronic final states plays an important role in the understanding of CP violation in the B system. In the Standard Model, CP violation arises from a single complex phase in the Cabibbo-Kobayashi-Maskawa (CKM) quark-mixing matrix V [1]. Measurements of the time-dependent CP -violating asymmetry in the $B^0 \rightarrow \pi^+\pi^-$ decay mode by the BABAR and Belle collaborations [2] provide information on the angle $\alpha \equiv \arg[-V_{td}V_{tb}^*/V_{ud}V_{ub}^*]$ of the unitarity triangle. However, in contrast to the theoretically clean determination of the angle β in B^0 decays to charmonium plus neutral-kaon final states [3, 4], the extraction of α in $B^0 \rightarrow \pi^+\pi^-$ is complicated by the interference of amplitudes with different weak phases. The difference between α_{eff} , derived from the measured $B^0 \rightarrow \pi^+\pi^-$ asymmetry, and α may be evaluated using isospin relations between the amplitudes for the decays $B^0(\bar{B}^0) \rightarrow \pi^+\pi^-$, $B^0(\bar{B}^0) \rightarrow \pi^0\pi^0$, and $B^\pm \rightarrow \pi^\pm\pi^0$ [5].

The primary contributions to the decay $B^0 \rightarrow \pi^0\pi^0$ are expected to come from the so-called color-suppressed tree and gluonic penguin amplitudes [6]. The branching fraction for $B^0 \rightarrow \pi^0\pi^0$ has been calculated in various QCD models [7]. All models use as inputs the values of the CKM angles, typically taken from unitarity-triangle fits. The predictions for $\mathcal{B}(B^0 \rightarrow \pi^0\pi^0)$ are in the range $(0.3 - 1.1) \times 10^{-6}$.

In this paper, we report the observation of the decay $B^0 \rightarrow \pi^0\pi^0$ based on $(124 \pm 1) \times 10^6 \Upsilon(4S) \rightarrow B\bar{B}$ pairs (on-resonance), collected with the BABAR detector. We also use approximately 12 fb^{-1} of data recorded 40 MeV below the $B\bar{B}$ threshold (off-resonance).

BABAR is a solenoidal detector optimized for the asymmetric-energy beams at PEP-II and is described in detail in Ref. [8]. Charged particle (track) momenta are measured with a 5-layer double-sided silicon vertex tracker and a 40-layer drift chamber inside a 1.5-T superconducting solenoidal magnet. Neutral cluster (photon) positions and energies are measured with an electromagnetic calorimeter (EMC) consisting of 6580 CsI(Tl) crystals. The photon energy resolution is $\sigma_E/E = \{2.3/E(\text{GeV})^{1/4} \oplus 1.9\} \%$, and the angular resolution from the interaction point is $\sigma_\theta = 3.9^\circ/\sqrt{E(\text{GeV})}$. The photon energy scale is determined using symmetric $\pi^0 \rightarrow \gamma\gamma$ decays. Charged hadrons are identified with a detector of internally reflected Cherenkov light and ionization in the tracking detectors. The instrumented magnetic-flux return detects neutral hadrons and identifies muons. High efficiency for recording $B\bar{B}$ events in which one B decays with low multiplicity is achieved with a two-level trigger with complementary tracking-based and calorimetry-based trigger decisions.

Candidate π^0 mesons are reconstructed as pairs of photons, spatially separated in the EMC, with an invariant

mass within 3σ of the π^0 mass. The mass resolution σ is approximately $8 \text{ MeV}/c^2$ for high-momentum π^0 mesons. Photon candidates are required to be consistent with the expected lateral shower shape, not to be matched to a track, and to have a minimum energy of 30 MeV. To reduce the background from false π^0 candidates, the angle θ_γ between the photon momentum vector in the π^0 rest frame and the π^0 momentum vector in the laboratory frame is required to satisfy $|\cos\theta_\gamma| < 0.95$.

B meson candidates are reconstructed by combining two π^0 candidates. Two kinematic variables, used to isolate the $B^0 \rightarrow \pi^0\pi^0$ signal, take advantage of the kinematic constraints of B mesons produced at the $\Upsilon(4S)$. The first is the beam-energy-substituted mass $m_{\text{ES}} = \sqrt{(s/2 + \mathbf{p}_i \cdot \mathbf{p}_B)^2/E_i^2 - \mathbf{p}_B^2}$, where \sqrt{s} is the total e^+e^- center-of-mass (CM) energy. (E_i, \mathbf{p}_i) is the four-momentum of the initial e^+e^- system and \mathbf{p}_B is the B candidate momentum, both measured in the laboratory frame. The second variable is $\Delta E = E_B - \sqrt{s}/2$, where E_B is the B candidate energy in the CM frame. The ΔE resolution for signal is approximately 80 MeV.

The primary source of background is $e^+e^- \rightarrow q\bar{q}$ ($q = u, d, s, c$) events where a π^0 from each quark jet randomly combine to mimic a B decay. The jet-like $q\bar{q}$ background is suppressed by requiring that the angle θ_s between the sphericity [9] axes of the B candidate and of the remaining tracks and photons in the event, in the CM frame, satisfies $|\cos\theta_s| < 0.7$. The other source of background is $B^\pm \rightarrow \rho^\pm\pi^0$ ($\rho^\pm \rightarrow \pi^\pm\pi^0$) decays in which the charged pion is emitted nearly at rest in the B rest frame so that the remaining two π^0 mesons are kinematically consistent with a $B^0 \rightarrow \pi^0\pi^0$ decay. Energy resolution smearing causes some $B^\pm \rightarrow \rho^\pm\pi^0$ events to have ΔE above the kinematic limit of $m_B - m_\pi$. From simulation, other B decays contribute no more than one background event.

The number of signal $B^0 \rightarrow \pi^0\pi^0$ candidates is determined in an extended, unbinned maximum-likelihood fit. The variables used in the fit are m_{ES} , ΔE , and a Fisher discriminant F . The F discriminant is a linear combination of three variables, optimized to separate signal from $q\bar{q}$ background. The first two variables are sums: $L_0 = \sum_i p_i$ and $L_2 = \sum_i p_i \cos^2\theta_i$ where p_i is the momentum and θ_i is the angle with respect to the thrust axis of the B candidate, both in the CM frame, for all tracks and neutral clusters not used to reconstruct the B meson. The third variable in F is the output of a neural network designed to separate B events from $q\bar{q}$ background, whose inputs are information from the remaining tracks and photons in the event. The inputs include information about high-momentum leptons, low-momentum leptons, charged kaons, and slow pions (from $D^{*+} \rightarrow D^0\pi_{\text{slow}}^+$) in the event; these are the same inputs used in the B -tagging algorithm of Ref. [3]. All neural-

network training and Fisher-discriminant optimization is performed using simulated events.

The data are divided into two samples: a signal sample with candidates satisfying $m_{\text{ES}} > 5.2 \text{ GeV}/c^2$ and $|\Delta E| < 0.2 \text{ GeV}$, and a sideband sample with candidates from on-resonance data with $m_{\text{ES}} > 5.2 \text{ GeV}/c^2$ and $0.2 < |\Delta E| < 0.4 \text{ GeV}$ (and well outside the triangular region in m_{ES} and ΔE populated by $B^\pm \rightarrow \rho^\pm \pi^0$ decays) and candidates from off-resonance data with $m_{\text{ES}} > 5.2 \text{ GeV}/c^2$ and $|\Delta E| < 0.4 \text{ GeV}$. The sideband sample contains only $q\bar{q}$ background candidates and is used in the fit to improve the statistical precision of the F distribution for $q\bar{q}$ events. There are 4470 events in the signal sample and 3253 events in the sideband sample. The reconstruction efficiency for $B^0 \rightarrow \pi^0 \pi^0$ is $(17.7 \pm 2.7)\%$, and for $B^\pm \rightarrow \rho^\pm \pi^0$ is $(0.8 \pm 0.1)\%$, derived from simulation. The errors are due to a systematic uncertainty in the efficiency for high-momentum π^0 mesons to pass the selection criteria.

For candidates in the signal sample the probabilities $\mathcal{P}_i(\vec{x}_j; \vec{\alpha}_i)$ used in the maximum-likelihood fit are the product of probability density functions (PDFs) for the variables $\vec{x}_j = \{m_{\text{ES}}, \Delta E, F\}$, given the set of parameters $\vec{\alpha}_i$. The likelihood function is given by a product over all $j = 1 - N$ candidates and a sum over the $i = \{B^0 \rightarrow \pi^0 \pi^0, B^\pm \rightarrow \rho^\pm \pi^0, q\bar{q}\}$ hypotheses:

$$\mathcal{L} = \exp \left(- \sum_{i=1}^3 n_i \right) \prod_{j=1}^N \left[\sum_{i=1}^3 n_i \mathcal{P}_i(\vec{x}_j; \vec{\alpha}_i) \right]. \quad (1)$$

The coefficients n_i are the numbers of $B^0 \rightarrow \pi^0 \pi^0$ signal, $B^\pm \rightarrow \rho^\pm \pi^0$ background, and $q\bar{q}$ background events in the sample. The number of $B^\pm \rightarrow \rho^\pm \pi^0$ events is fixed in the fit to the expected value based on the measured branching fraction $\mathcal{B}(B^\pm \rightarrow \rho^\pm \pi^0) = (11.0 \pm 2.7) \times 10^{-6}$ [10]. For candidates in the sideband sample, the likelihood function includes only the PDF for the F variable, and only the component for $q\bar{q}$ background. A simultaneous fit to both signal sample and sideband sample data is performed. Monte Carlo simulations are used to verify that the likelihood fit is unbiased.

The PDFs are determined from data and simulation. The m_{ES} and ΔE variables are correlated for both $B^0 \rightarrow \pi^0 \pi^0$ and $B^\pm \rightarrow \rho^\pm \pi^0$, so a two-dimensional PDF derived from a smoothed, simulated distribution is used. The m_{ES} distribution for $q\bar{q}$ events is modeled as a threshold function [11] whose shape parameter is determined from data with $|\cos \theta_s| > 0.9$. The ΔE distribution for $q\bar{q}$ events is modeled as a quadratic polynomial with parameters determined from data with $m_{\text{ES}} < 5.26 \text{ GeV}/c^2$.

The PDF for the F variable is modeled as a parametric step function (PSF) for $B^0 \rightarrow \pi^0 \pi^0$, $B^\pm \rightarrow \rho^\pm \pi^0$, and $q\bar{q}$ events. A PSF is a binned distribution (as in a histogram), whose parameters are the heights of each bin. Since the parent distribution of F is not known, any functional form (such as a multiple Gaussian) assumed

for the PDF will suffer from a systematic uncertainty due to the choice of function. By binning the data, the PSF substantially reduces this uncertainty. The PSF is normalized to one, so that the number of free parameters is the number of bins minus one. For both $B^0 \rightarrow \pi^0 \pi^0$ and $B^\pm \rightarrow \rho^\pm \pi^0$, the F PSF parameters are taken from a sample of 3.2×10^4 fully reconstructed $B^0 \rightarrow D^{(*)} n \pi$ ($n = 1, 2, 3$) events in data. The F PSF has ten bins, with bin limits chosen so that each bin contains approximately 10% of the $B^0 \rightarrow D^{(*)} n \pi$ events. Simulation is used to verify that the same distribution can be used for both $B^0 \rightarrow \pi^0 \pi^0$ and $B^\pm \rightarrow \rho^\pm \pi^0$. For $q\bar{q}$ background, the F PSF parameters are free parameters in the fit; these parameters are determined from data in both the signal and sideband samples.

All event-selection requirements, PDF parameters, and maximum-likelihood fit conditions were determined before fitting the data.

The result of the fit is $n_{B^0 \rightarrow \pi^0 \pi^0} = 46 \pm 13$ events, corresponding to a branching fraction of $\mathcal{B}(B^0 \rightarrow \pi^0 \pi^0) = (2.1 \pm 0.6) \times 10^{-6}$. B^0 and \bar{B}^0 decays are not separated, so the branching fraction is measured for the average of B^0 and \bar{B}^0 . The m_{ES} , ΔE , and F distributions are shown in Fig. 1 for all data used in the fit, and in Fig. 2 for events that pass a requirement on the signal probability ratio. This requirement is optimized to maximize the ratio $S/\sqrt{S+B}$, where S is the number of signal events and B is the number of background events in the plot. The significance of the change in $-2 \ln \mathcal{L}$ between the nominal fit and a separate fit in which the signal yield is fixed to zero, and is found to be 4.7σ with statistical errors only.

The number of signal events is stable when the $q\bar{q}$ m_{ES} and ΔE PDF parameters, or $n_{B^\pm \rightarrow \rho^\pm \pi^0}$, are allowed to vary in the fit. A validation of the maximum-likelihood fit is made by performing a simpler event-counting analysis, based on the number of events satisfying tighter m_{ES} , ΔE , and F requirements. The event-counting analysis finds 13 ± 6 events with an efficiency of 31% relative to the maximum-likelihood fit. This agrees well with the fitted result, and has a statistical significance of 2.7σ .

This result is consistent with our previous limit for this decay [12] based on $88 \times 10^6 B\bar{B}$ pairs. The data described in Ref. [12] were reanalyzed with improved EMC energy calibration and tracking alignment. More events are observed in this data sample after the reanalysis, consistent with the improved understanding of the detector.

Systematic uncertainties on the event yield are evaluated by varying the fixed parameters and refitting the data, and are summarized in Table I. The shape parameter for the threshold function describing the m_{ES} distribution for $q\bar{q}$ events is varied to account for the statistical error from the fit to the sample with $|\cos \theta_s| > 0.9$ and the extrapolation from $|\cos \theta_s| > 0.9$ to $|\cos \theta_s| < 0.7$. The $q\bar{q}$ ΔE polynomial parameters are varied by their statistical errors. The number of $B^\pm \rightarrow \rho^\pm \pi^0$ back-

ground events is varied according to the uncertainties on the $B^\pm \rightarrow \rho^\pm \pi^0$ branching fraction and reconstruction efficiency. Finally, the uncertainty in the mean of the ΔE distribution for $B^0 \rightarrow \pi^0 \pi^0$ is evaluated from a study of $B^\pm \rightarrow \rho^\pm \pi^0$ events that have a high momentum π^0 . Extrapolating from the uncertainty in the mean ΔE for this sample, we vary the mean of ΔE by ± 12 MeV to evaluate the systematic uncertainty on the signal yield. The effect of these uncertainties on the significance of the event yield is evaluated by choosing the variation that reduces the signal in all four systematic effects, and then refitting the data. The significance of the signal yield after accounting for systematic uncertainties is 4.2σ . The change in $-2 \ln \mathcal{L}$ as a function of the signal event yield is shown in Fig. 2d.

We observe $46 \pm 13 \pm 3$ $B^0 \rightarrow \pi^0 \pi^0$ events with a significance of 4.2 standard deviations including systematic uncertainties. We measure a branching fraction $\mathcal{B}(B^0 \rightarrow \pi^0 \pi^0) = (2.1 \pm 0.6 \pm 0.3) \times 10^{-6}$, where the first error is statistical and the second is systematic. The branching fraction is an average for B^0 and \bar{B}^0 decays. The systematic uncertainties from PDF variations and efficiency have been combined in quadrature. This result is consistent with, and supersedes, our previous limit for this decay [12]; it is also consistent with other prior limits [13]. The observed $B^0 \rightarrow \pi^0 \pi^0$ branching fraction is larger than predicted theoretically.

TABLE I: A summary of systematic uncertainties listed as the change in the fitted event yield, $\Delta n_{B^0 \rightarrow \pi^0 \pi^0}$, for different parameter variations.

Parameter	$\Delta n_{B^0 \rightarrow \pi^0 \pi^0}$
$q\bar{q}$ m_{ES} shape parameter	± 2.0
$q\bar{q}$ ΔE quadratic polynomial	$+0.9$ -1.0
$n_{B^\pm \rightarrow \rho^\pm \pi^0}$	± 0.9
$B^0 \rightarrow \pi^0 \pi^0 \Delta E$ mean	$+0.6$ -1.0

We are grateful for the excellent luminosity and machine conditions provided by our PEP-II colleagues, and for the substantial dedicated effort from the computing organizations that support BABAR. The collaborating institutions wish to thank SLAC for its support and kind hospitality. This work is supported by DOE and NSF (USA), NSERC (Canada), IHEP (China), CEA and CNRS-IN2P3 (France), BMBF and DFG (Germany), INFN (Italy), FOM (The Netherlands), NFR (Norway), MIST (Russia), and PPARC (United Kingdom). Individuals have received support from the A. P. Sloan Foundation, Research Corporation, and Alexander von Humboldt Foundation.

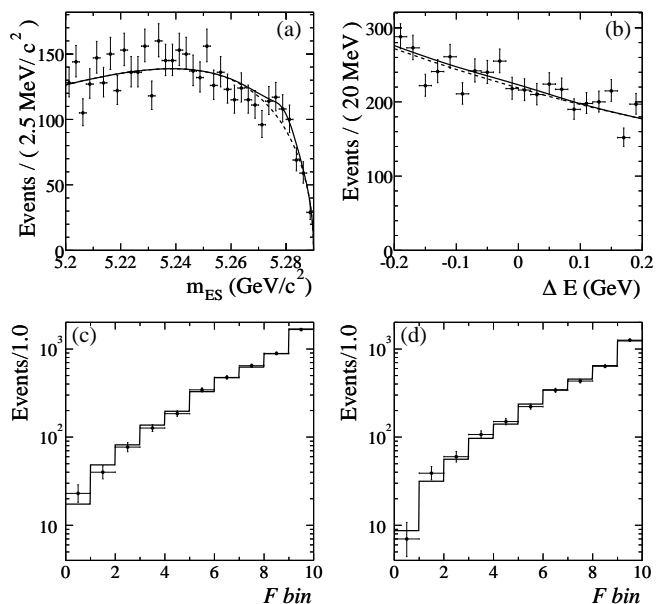


FIG. 1: The distributions of a) m_{ES} , b) ΔE , and c) Fisher discriminant F for candidates in the signal data sample, and d) the F distribution for candidates in the sideband data sample. The solid lines show the PDF for signal plus background. For m_{ES} and ΔE , the dashed lines show the PDF for the $q\bar{q}$ background. The abscissa in c) and d) is the F bin number, where the bins have been chosen so that each bin contains approximately 10% of the distribution for the $B^0 \rightarrow D^{(*)} n \pi$ data sample.

* Also with Università di Perugia, Perugia, Italy

† Also with Università della Basilicata, Potenza, Italy

‡ Also with IFIC, Instituto de Física Corpuscular, CSIC-Universidad de Valencia, Valencia, Spain

§ Deceased

- [1] N. Cabibbo, Phys. Rev. Lett. **10**, 531 (1963); M. Kobayashi and T. Maskawa, Prog. Th. Phys. **49**, 652 (1973).
- [2] BABAR Collaboration, B. Aubert *et al.*, Phys. Rev. Lett. **89**, 281802 (2002); Belle Collaboration, K. Abe *et al.*, Phys. Rev. D **68**, 012001 (2003).
- [3] BABAR Collaboration, B. Aubert *et al.*, Phys. Rev. Lett. **89**, 201802 (2002).
- [4] Belle Collaboration, K. Abe *et al.*, Phys. Rev. D **66**, 071102 (2002).
- [5] M. Gronau and D. London, Phys. Rev. Lett. **65**, 3381 (1990).
- [6] M. Gronau, O. Hernandez, D. London, and J.L. Rosner, Phys. Rev. D **50**, 4529 (1994).
- [7] M. Beneke, G. Buchalla, M. Neubert, and C.T. Sachrajda, Nucl. Phys. B **606**, 245 (2001); M. Ciuchini, E. Franco, G. Martinelli, M. Pierini, and L. Silvestrini, Phys. Lett. B **515**, 33 (2001); D. Du, J. Sun, D. Yang, and G. Zhu, Phys. Rev. D **67**, 014023 (2003); Y.-Y. Keum and A.I. Sanda, Phys. Rev. D **67**, 054009 (2003).

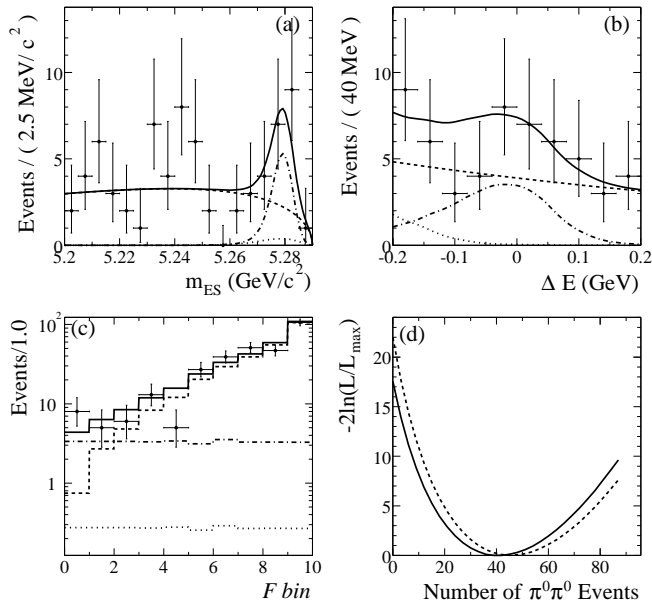


FIG. 2: The distributions of a) m_{ES} , b) ΔE , and c) Fisher discriminant F for candidates in the signal data sample that satisfy an optimized requirement on the signal probability, based on all variables except the one being plotted. The fraction of signal events included in the plots is 24%, 42% and 74% for m_{ES} , ΔE , and F , respectively. The PDF projections are shown as a dashed line for $q\bar{q}$ background, a dotted line for $B^\pm \rightarrow \rho^\pm \pi^0$, and a dashed-dotted line for $B^0 \rightarrow \pi^0 \pi^0$ signal. The solid line shows the sum of all PDF projections. The PDF projections are scaled by the expected fraction of events passing the probability-ratio requirement. The ratio $-2\ln(L/L_{max})$ is shown in d) where the dashed line corresponds to statistical errors only and the solid line corresponds to statistical and systematic errors, as applied for the calculation of significance.

- [8] BABAR Collaboration, B. Aubert *et al.*, Nucl. Instr. Meth. A **479**, 1 (2002).
- [9] G. Hanson *et al.*, Phys. Rev. Lett. **35**, 1609 (1975).
- [10] BABAR Collaboration, B. Aubert *et al.*, BABAR-CONF-03/14 (2003).
- [11] The threshold function used for the m_{ES} PDF is $(m_{ES}/m_0)\sqrt{1-(m_{ES}/m_0)^2}\exp\{-\xi[1-(m_{ES}/m_0)^2]\}$, where m_0 is the m_{ES} endpoint, and ξ the shape parameter. See ARGUS Collaboration, H. Albrecht *et al.*, Z. Phys. C **48**, 543 (1990).
- [12] BABAR Collaboration, B. Aubert *et al.*, Phys. Rev. Lett. **91**, 021801 (2003).
- [13] CLEO Collaboration, A. Bornheim *et al.*, CLNS-03-1816, CLEO-03-03, hep-ex/0302026, submitted to Phys. Rev. D; Belle Collaboration, B.C.K. Casey *et al.*, Phys. Rev. D **66**, 092002 (2002).